THE REDDENING LAW OUTSIDE THE LOCAL GROUP GALAXIES: THE CASE OF NGC 7552 AND NGC 5236

ANNE L. KINNEY[1,2] AND DANIELA CALZETTI[1]
Space Telescope Science Institute, 3700 San Martin Drive, Baltimore, MD 21218

AND

EDUARDO BICA AND THAISA STORCHI-BERGMANN[2]
Instituto de Física, Universidade Federal do Rio Grande do Sul, C.P. 15051, Porto Alegre, RS, 91501-970, Brazil

ABSTRACT

The dust reddening law from the UV to the near-IR for the extended regions of galaxies is here derived from the spectral distributions of the starburst spiral galaxies NGC 7552 and NGC 5236. The centers of these galaxies have similar absorption and emission line spectra, differing only in the strength of their interstellar lines and in the continuum distribution, with NGC 7552 appearing more reddened than NGC 5236. The disk of NGC 7552 is more inclined, and there is evidence that its center is observed through additional foreground dust and gas clouds, as compared to the center of NGC 5236. While the galaxies can be expected to have similar dust *content*, they are known to have different dust *path lengths* to our line of sight. Therefore, differences in the shape of the spectra can be attributed mainly to the effects of dust, allowing us to probe for the first time the properties of the reddening law outside the local group of galaxies. We derive the reddening law based on the optical depth of the emission lines of Hα and Hβ and also based on the continuum distribution. We find that the optical depth from the emission line regions are about twice the optical depth of the continuum regions. Thus, dereddening a starburst galaxy by scaling the Milky Way reddening laws to optical depths obtained from the Hα/Hβ line ratio overcompensates for the effect of dust.

Subject headings: dust, extinction — galaxies: individual (NGC 5236, NGC 7552) — galaxies: ISM — galaxies: starburst — ultraviolet: galaxies

1. INTRODUCTION

The Milky Way, LMC, and SMC are the only three galaxies for which a reddening law has been determined because of the intrinsic difficulty in observing stars in external galaxies. The UV reddening laws for the three systems are quite different, with the 2175 Å dust feature weakening and the UV slope increasing, constituting a sequence from the Milky Way, to the LMC to the SMC. The difference has been attributed to variations in the composition of dust due to the different metallicities of the three galaxies (Lequeux 1988), but this interpretation is difficult to verify.

Reddening laws show a wide dispersion of properties even within the Milky Way (Witt, Bohlin, & Stecher 1984). In addition, the *extinction* determined by observing a known spectral type of star through different path lengths may be very different than the *attenuation* one would observe in the extended regions of galaxies: scattering and the geometrical distribution of dust relative to the distribution of hot stars can greatly influence the appearance of the emerging flux. Indeed, Witt, Thronson, & Capuano (1992), Bruzual, Magris, & Calvet (1988), and Natta & Panagia (1984) have shown that scattering and geometrical distribution of dust play an important role in weakening the 2175 Å dust feature and in causing the "attenuation" curve to be gray, i.e., approximately constant

with wavelength. These works point out that the details of the reddening correction of extended regions depends on their particular geometrical configuration. An important clue to the attenuation due to dust outside our local group is the absence of the 2175 Å bump in the UV spectra of quasars (Kinney et al. 1991), damped Lyα systems (Pei, Fall, & Bechtold 1991), and, especially, galaxies (Kinney et al. 1993).

We derive a reddening law for galaxies using the method applied to stars—the ratioing of the spectrum of a highly reddened object with the spectrum of a less unreddened object (Witt et al. 1984). With two galaxies well matched by physical properties but lying at different inclination angles, we form the ratio of the spectrum of the face-on galaxy with the spectrum of the more edge-on galaxy, thus deriving the wavelength dependence of the reddening law.

NGC 7552 and NGC 5236 have been chosen because they are undergoing a burst of star formation, thus providing a strong flux in the UV and because they are well matched both morphologically and, as discussed below, by stellar population. Both are grand design barred spirals; emission from a spiral which is "edge-on" must cross a longer path length of dust and gas than emission from a "face-on" spiral. This effect has been observed in the interstellar NaI D feature (Bica & Alloin 1986, hereafter BA86; Bica et al. 1991). NGC 5236 is nearly face-on, the axial ratio suggesting an inclination of $i \approx 24°$. The axial ratio for NGC 7552 is very dependent on the isophotal level (de Vaucouleurs, de Vaucouleurs, & Corwin 1976; Durret & Bergeron 1987; Lauberts & Valentijn 1989): those of the bright disk imply possible inclinations in the range $i \approx 35°-65°$, whereas the outer faint arms might suggest nearly face-on orientation. Consequently, dust and gas clouds in this

disk probably lie in front of the NGC 7552 nucleus, which is not the case for NGC 5236. The foreground clouds are surmised from the following observations; (i) the bright disk has extended diffuse ionized regions with an asymmetry in the outer parts toward the S-E direction, possibly related to a past interaction with other members of the Grus quartet (Durret & Bergeron 1987); (ii) NGC 7552 contains a dust ring around the central parts, an extended dusty structure toward the S-E, and a highly asymmetric H I profile which shows a possible broad absorption component, redshifted (and thus apparently accreting) by some 300 km s^{-1} with respect to the systemic velocity of the galaxy (Feinstein et al. 1990, Reif et al. 1982); (iii) the absorption feature NaI is much stronger in NGC 7552 than in NGC 5236, denoting a larger interstellar gas column density (BA86).

The two galaxies are in the sample of Bica & Alloin (1987, hereafter BA87), observed through a small aperture (5″ × 8″) in the visible spectral range. Assuming a Milky Way reddening law, and taking into account the Milky Way reddening in front of NGC 5236, an additional reddening of $E(B-V) = 0.18$ was derived for the region in front of the burst region of NGC 7552 based on the difference in spectral shape between the two galaxies. Because of their similar stellar absorption spectra, the two galaxies are included in the same classification in Bica (class S7, 1988), for which the population synthesis indicated that their starbursts are not a single stellar generation associated with the emission lines, but have been bursting for at least 100 Myr. The emission line spectra, after the correction of the extranuclear sources of reddening and the subtraction of the underlying stellar population, have strong Balmer decrements, indicating that considerable reddening occurs in the line-emitting regions (Bonatto, Bica, & Alloin 1989). The emission lines are typical of metal rich nuclear H II regions. Indeed, many hot spots are present in the central parts of NGC 5236 and NGC 7552 (Sérsic & Pastoriza 1965; Pastoriza 1975).

In the present paper we report UV and optical spectra, obtained in large, matched apertures between the UV and optical ranges and covering the wavelength range 1200–10,000 Å. The two objects are part of a larger program aimed at studying the impact of dust on the spectrum, stellar content, Initial Mass Function and Star Formation Rates from a large sample of UV and optical spectra of starburst and Blue Compact galaxies (see Kinney et al. 1993, Calzetti, Kinney, & Storchi-Bergmann 1994, and Storchi-Bergmann, Kinney, & Challis 1994b).

2. OBSERVATIONS AND DATA ANALYSIS

The UV spectra of the NGC 7552 and NGC 5236 are archival *IUE* spectra collected in the Atlas of Kinney et al. (1993), with the spectrum of NGC 5236 updated to include recently released data. The optical spectra were obtained during May, June, and November of 1992 at the CTIO 1 m

telescope with the "2D FRUTTI" detector for the visible range and at the 1.5 m telescope with a CCD detector for the near-IR. A long slit with a 10″ width was used, and a window 20″ long was extracted to match the 10″ × 20″ *IUE* aperture. The CTIO spectra cover the wavelength range 3200–10,000 Å with a resolution ~8 Å (observations are reported in detail in Storchi-Bergmann et al. 1994b).

The emission lines of the Balmer series, Hα and Hβ, have been measured to determine the total color excess, Milky Way plus galactic, $[E(B-V)]$, using the reddening law of Seaton (1979) and assuming an average underlying stellar absorption of 2 Å (McCall, Rybski, & Shields 1985). This preliminary value of the reddening has been used to deredden the metallic emission lines of [O II] λ3727, [N II] λ6584 and [S II] λλ6717, 6731, in order to determine the electron temperature and density, which are then used to derive the oxygen abundance (discussed in detail in Storchi-Bergmann, Calzetti, & Kinney 1994a).

Table 1 lists the relevant information concerning the two galaxies: the galaxy name, the morphological type, the redshift, the color excess due to extinction from the Milky Way $[E(B-V)_{MW}$, see Burstein & Heiles 1984], the total color excess determined from the Balmer line ratio, the oxygen abundance, and the derived values of electron temperature T_e and electron density N_e.

The original spectra have been corrected for the spikes at the ends of the *IUE* SWP and LWP spectral ranges, and NGC 5236 has been corrected for its small Milky Way reddening using Seaton's (1979) law. The spectra are shown in Figure 1.

3. DISCUSSION

3.1. *The Intrinsic Stellar Population*

The galaxies lie at different distances, so that our fixed aperture corresponds to 0.4 kpc × 0.8 kpc at NGC 5236 and 1.8 kpc × 3.7 kpc at NGC 7552 ($H_0 = 50$ km s^{-1} Mpc^{-1}). Nevertheless, the spectral features from the stellar population are similar in the two galaxies, both in our large apertures and in those of BA87, showing that the stellar population mixture does not change significantly with radius. In the present spectra, the measured values of the equivalent widths are (Storchi-Bergmann et al. 1994b): $W(\text{Si IV}) = 11.3$ Å, $W(\text{C IV}) = 12.3$ Å, $W(\text{Ca II-K}) = 4.4$ Å, $W(\text{MgI} + \text{MgH}) = 1.3$ Å, $W(\text{NaI}) = 2.3$ Å for NGC 5236 and $W(\text{Si IV}) = 10.2$ Å, $W(\text{C IV}) = 11.5$ Å, $W(\text{Ca II-K}) = 4.6$ Å, $W(\text{MgI} + \text{MgH}) = 1.8$ Å, $W(\text{NaI}) = 4.6$ Å for NGC 7552. Thus, the values for equivalent width are similar (see also Fig. 1), denoting comparable metallicity and age distribution for the stellar population (BA87, Bica 1988), except for NaI, which, owing to the interstellar component shows, a larger equivalent width for the more reddened NGC 7552 (BA86).

The two galaxies also have similar nebular emission lines (Fig. 1). The presence of the lines indicates that massive ion-

TABLE 1

GALACTIC PARAMETERS

Name	Type	Redshift	$E(B-V)_{MW}$[a]	$E(B-V)_t$[b]	O[c]	T_E (K)	N_e (cm^{-3})
NGC 5236	SBc	0.00174	0.03	0.33	>9.3	<3700	280
NGC 7552	SBbc	0.00531	0.00	0.70	>9.0	<4500	360

[a] Color excess due to the Milky Way; Burstein & Heiles 1984.
[b] Color excess determined from Balmer line ratios.
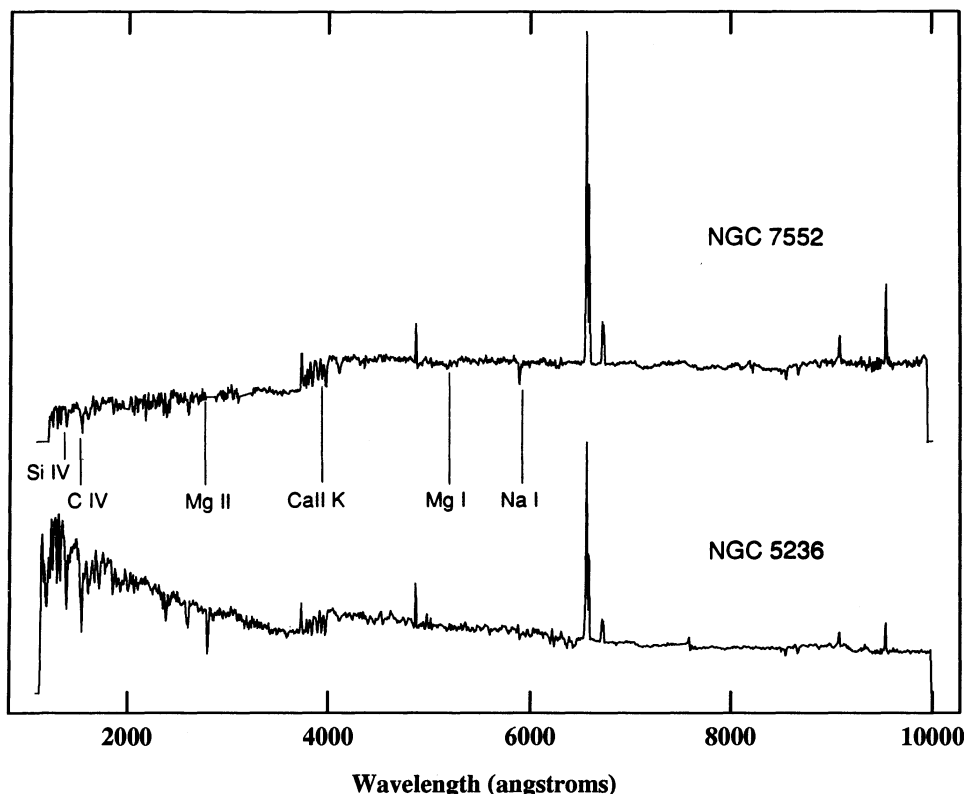[c] Oxygen abundance: 12 + log (O/H).

Fig. 1.—Two spectra of NGC 5236 (*bottom*) and NGC 7552 (*top*) are plotted in the range 1250–10,000 Å. The region around Mg II in NGC 7552 has been contaminated by the readout of the *IUE*.

izing stars must still be present, requiring that at least part of the burst is younger than $\approx 3 \times 10^7$ yr (Bruzual & Charlot 1993). During the first 3×10^7 yr of a burst, the UV continuum in the range 1200–2000 Å, which is due mainly to B stars, does not undergo much evolution. In addition, the two galaxies have similar values of oxygen abundance (Storchi-Bergmann et al. 1994b), indicating that there is little difference in the burst IMF's. Therefore, we conclude that the populations due to the current burst of star formation in the two galaxies are similar.

The relative proportion between stars earlier and later than A is given by the intensity of the Balmer jump at $\lambda \sim 3600$ Å. Accounting for the difference in reddening between NGC 7552 and NGC 5236, the Balmer jump is within 12% in the two galaxies, suggesting that the ratio between the long lived F and G stars and the relatively short lived O and B stars is comparable. The small difference in the Balmer jump is most likely due to the additional bulge population included in the aperture of the more distant galaxy, NGC 7552.

These arguments indicate that the differences in spectral shape between NGC 7552 and NGC 5236 are not dominated by differences in the stellar populations of the two galaxies. The origin of the differences in spectral shape and in the interstellar NaI in NGC 7552 appears to be due to the overlying layer of clouds from the inclined disk in NGC 7552.

3.2. *The Derivation of the Reddening Law*

The UV spectra of two galaxies with similar morphology, similar stellar content, and similar ages but with different inclination to the line of sight can be used to derive a galactic reddening law in much the same way as the spectra of two stars of similar spectra type and similar luminosity class but differ-

ent color excess are used to derive the Galactic reddening law. Reddening curves are parameterized by the wavelength dependence, $k(\lambda)$ [where the Seaton (1979) law is the standard in the UV] scaled by the color excess $E(B-V)$. As long as there is a *difference* in the scaling factor for the two objects, $E(B-V)$, the wavelength dependence of the reddening, $k(\lambda)$, can be determined by the ratio of the fluxes of the two objects. The assumption that we invoke, that dust is in the form of an overlying screen, will always cause an overestimate of the amount of dust (i.e., the scaling factor) if dust is in fact in a more complex geometry, but the derivation of wavelength dependence will still be valid.

We want here to derive the shape of the reddening—but the quantity which we can calculate directly is the *product* of $E(B-V)$ and $k(\lambda)$, or $\tau(\lambda)$. In the case of an overlying screen, $\tau(\lambda)$ is given by

$$\tau(\lambda) = 0.921 \times E(B-V) \times k(\lambda) , \tag{1}$$

and in our case by

$$\tau(\lambda) = -\ln\frac{F_{7552}(\lambda)}{F_{5236}(\lambda)} + C . \tag{2}$$

This yields the difference in optical depths for the continua of the two galaxies, since $\tau(\lambda)$ is based on the ratio of the continuum fluxes.

For the purpose of deriving the shape of the reddening law, we have excluded the regions of the interstellar absorption lines from the spectra of the two galaxies in the range 1250–1400 Å. The spectra of NGC 5236 and NGC 7552 have been smoothed in bins of 50 Å. The fit to equation (2) has been performed in the range 1250–3900 Å, using a polynomial fit.

For the region at wavelengths longer than 3900 Å, the usual LMC fit scaled by an appropriate factor provides an accurate description of the reddening law. In particular, for $\lambda < 3900$ Å:

$$\tau(\lambda) = -1.14 + 0.69x - 0.05x^2 + 0.002x^3 , \qquad (3)$$

where $x = 1/\lambda$. Assuming the parameterization given by Howarth (1983), the optical reddening law is given by

$$\tau(\lambda) = 0.22[2.30(x - 1.83) - 0.493(x - 1.83)^2]$$

$$\text{for } 3900 \leq \lambda \leq 5460$$

$$\tau(\lambda) = 0.22\{[(1.86 - 0.48x)x - 0.1]x - 3.1\}$$

$$\text{for } \lambda > 5460 .$$

The formal 1 σ uncertainty in the parameters is about 5%. However, there is an additional uncertainty of 12% in the region around 4000 Å due to the difference in the Balmer jump between the two galaxies. Figure 2 shows the fit overplotted onto normalized $\tau(\lambda)$ in the range 1250–10,000.

3.2.1. The Derivation Based on the Emission Line Optical Depth

We can measure the difference in optical depth in the two galaxies using the observed emission lines Hα and Hβ, assuming an intrinsic Balmer ratio Hα/Hβ = 2.87 (Osterbrock 1986) and correcting for the foreground MW extinction. We find $\tau_{\alpha,\beta}^{NGC\,5236} = 0.32$, and $\tau_{\alpha,\beta}^{NGC\,7552} = 0.75$. The difference in the optical depths of the emission lines is thus $\tau_{\alpha,\beta}^{line} = 0.43$. We can compare this value with that obtained from the continuum by measuring $\tau_{\alpha,\beta}$ directly from the $\tau(\lambda)$ curve, at the corresponding wavelengths of Hα and Hβ. We obtain $\tau_{\alpha,\beta}^{cont} = 0.23$, which is approximately half the value obtained from the emission lines.

Interestingly, in a statistical study of spectra of 40 star-forming nuclei, it is found that, on the average, $\tau_{\alpha,\beta}^{cont} = 0.5 \times \tau_{\alpha,\beta}^{line}$ (Calzetti et al. 1994; Storchi-Bergmann et al. 1994a). In the latter studies, this result is attributed to the fact that the reddening in the regions where the Balmer emission lines are being produced is higher than the reddening affecting the continuum. Hot, ionizing stars (earlier than type B1 or B2, which emit predominantly shortward of 1200 Å) would still be closely associated with the dusty, gaseous molecular clouds in which they were produced, while later type stars (later than B2, which emit predominantly longward of 1200 Å) can live long enough to drift far from the clouds in which they were born (Leisawitz
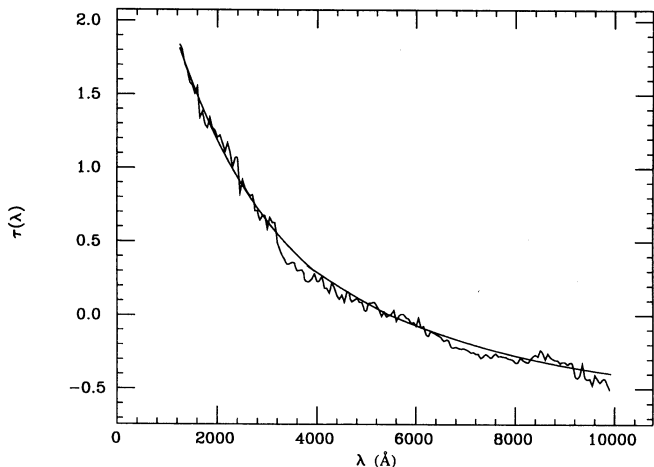

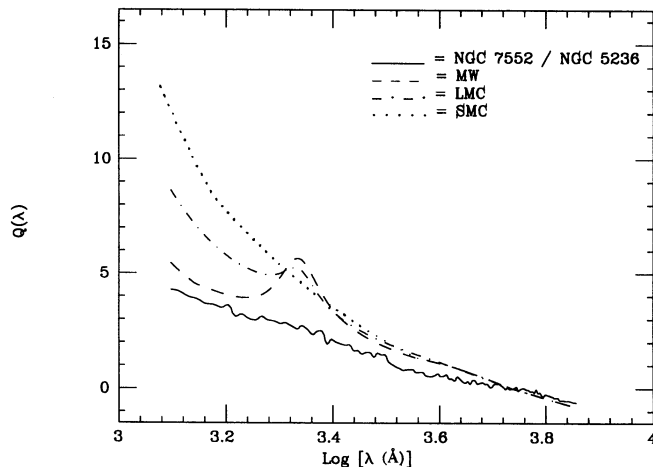FIG. 2.—Fit for $\tau(\lambda)$ is shown together with the data normalized to $\tau(5500$ Å$) = 0$.

FIG. 3.—$Q(\lambda)$, the optical depth normalized to $\tau_{\alpha,\beta}^{line} = 1$, is overplotted with the Milky Way, the LMC, and the SMC reddening laws. Note that the zero point of the galactic reddening is arbitrary relative to the reddening of the Milky Way, LMC, and SMC. This normalized optical depth can be used to deredden UV/optical spectra of galaxies given the optical depth of the galaxy based on the Balmer decrement.

& Hauser 1988). (Cardelli, Clayton, & Mathis 1989 also report that they find no unreddened star earlier than type O6, verifying the picture of early type stars living close to their birthplace.)

Thus, the gas is probing the largest observable optical depths, the continuum being less affected because it includes contributions of less obscured stars, which can be interpreted as a grayer reddening law (see below). Under this assumption, the parameterization of the reddening law is carried out by means of the emission line $\tau_{\alpha,\beta}^{line}$. We thus define:

$$Q(\lambda) = \frac{k(\lambda)}{(k_\beta - k_\alpha)} = \frac{\tau(\lambda)}{\tau_{\alpha,\beta}^{line}}$$

We show this result in Figure 3. We compare the latter curve to the Milky Way, LMC and SMC laws expressed in terms of $Q(\lambda)$. The derived law has a slope that is more gray than the stellar extinction curves, and showing no evidence of a 2175 Å absorption feature.

The 2175 Å bump in the Milky Way, LMC, and SMC is attributed to small graphite grains. The 2175 Å bump appears less prominent in H II regions with larger R-values (Cardelli et al. 1989; Fitzpatrick 1986), but never disappears altogether. The lack of bump may be due to coagulation of the small grains into larger grains thought to occur in regions of high density and high turbulence (Mathis 1990). Alternatively, the small graphite grains may be inhibited from forming in the starburst galaxies.

3.2.2. The Derivation Based on the Continuum Optical Depth

The known reddening laws—Milky Way, LMC, and SMC, are usually parameterized as

$$k(\lambda) = \frac{A(\lambda)}{E(B-V)} .$$

In the assumption that the dust obscuring the stellar population is all foreground, we can make an analogy with the case of stellar extinction and derive an effective $k(\lambda)$

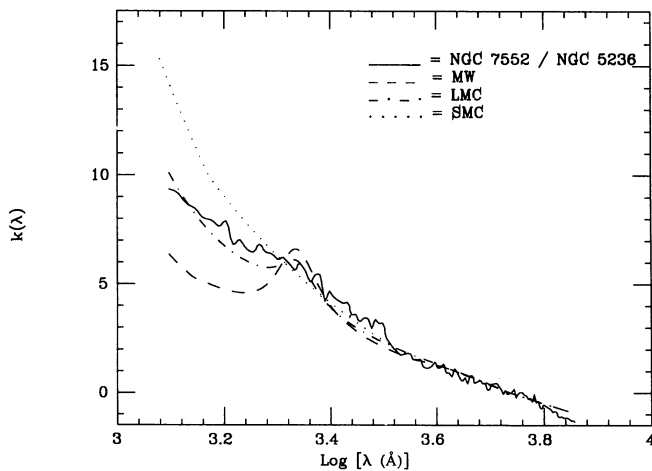$$k(\lambda) = \frac{\tau(\lambda)}{\tau_B - \tau_V} = \frac{A(\lambda)}{A_B - A_V} , \qquad (4)$$

FIG. 4.—$k(\lambda)$ is shown for the galaxies based on their continuum reddening compared with $k(\lambda)$ for the Milky Way, the LMC, and the SMC.

and impose, as in the case of stellar extinction, $k(B) - k(V) = 1.0$. From Figure 2, we have $\tau_B - \tau_V = 0.2$; the corresponding $k(\lambda)$ normalized by this value is shown in Figure 4, together with $k(\lambda)$ for the Milky Way, the SMC, and the LMC. While the overall slope of the reddening law resembles that of the LMC, there is no evidence for the 2175 Å absorption feature.

4. CONCLUDING REMARKS

We have studied, for the first time outside the Local Group Galaxies, the behavior of the reddening law from the UV to the near-IR for extended regions of galaxies. The optical depth of the emission line regions is approximately twice that of the continuum regions. When using an optical depth based on the Hα/Hβ line ratio and existing reddening laws, the effects of reddening on a starburst galaxy will be strongly overestimated.

The 2175 Å absorption bump observed in the Milky Way is conspicuously absent in our derived reddening law. Coagulation of small dust grains in a dense and turbulent gas may be the cause of the diminished 2175 Å dust feature (Mathis 1990).

The study of reddening laws affecting extended regions of galaxies requires careful disentangling of the different sources of reddening: (i) Milky Way foreground reddening (for NGC 5236); (ii) galactic dust intercepting emission through inclined or warped disks; (iii) galactic dust mixed with the stellar populations; (iv) galactic dust mixed with the gas in the line emitting regions. Disentangling the last three effects is not an easy task because it depends on the details of the geometrical distribution of the dust, and on the mixture of stellar populations of different ages.

Understanding the effects of extinction on galaxy emission is relevant for all work on distant galaxies, where the UV emission is redshifted into the optical. Given the importance of the effect of dust on galactic spectra in the UV, the reddening law is derived in Calzetti et al. (1994) based on templates of galaxies, in a manner complementary to the approach taken here.

REFERENCES

Bica, E. 1988, A&A, 195, 76
Bica, E., & Alloin, D. 1986, A&A, 166, 83 (BA86)
———. 1987, A&AS, 70, 281 (BA87)
Bica, E., Pastoriza, M., Maia, M., da Silva, L. A., & Dottori, H. 1991, AJ, 102, 1702
Bonatto, Ch., Bica, E., & Alloin, D. 1989, A&A, 226, 23
Bouchet, P., Lequeux, J., Maurice, E., Prevot, L., & Prevot-Burnichon, M. L. 1985, A&A, 149, 330
Bruzual, G. A., & Charlot, S. 1993, ApJ, 405, 538
Bruzual, G. A., Magris, G. C., & Calvet, N. 1988, ApJ, 333, 673
Burstein, D., & Heiles, C. 1984, ApJS, 54, 33
Calzetti, D., Kinney, A. L., & Storchi-Bergmann, T. 1994, ApJ, in press
Cardelli, J. A., Clayton, G. C., & Mathis, J. S. 1989, ApJ, 345, 245
de Vaucouleurs, G., de Vaucouleurs, A., & Corwin, H. G., Jr. 1976, Second Reference Catalogue of Bright Galaxies (Austin: Univ. Texas Press)
de Vaucouleurs, G., Pence, W. D., & Davoust, E. 1983, ApJS, 53, 17
Durret, F., & Bergeron, J. 1987, A&A, 173, 219
Feinstein, C., Vega, I., Mendez, M., & Forte, J. C. 1990, A&A, 239, 90
Fitzpatrick, E. L. 1986, AJ, 92, 1068
Howarth, I. D. 1983, MNRAS, 203, 301
Kinney, A. L., Bohlin, R. C., Blades, J. C., & York, D. G. 1991, ApJS, 75, 645
Kinney, A. L., Bohlin, R. C., Calzetti, D., Panagia, N., & Wyse, R. F. G. 1993, ApJS, 86, 5

Lauberts, A., & Valentijn, E. A. 1989, The Surface Photometry Catalogue of the ESO-Uppsala Galaxies (Garching: ESO)
Leisawitz, D., & Hauser, M. G. 1988, ApJ, 332, 954
Lequeux, J. 1988, in Dust in the Universe, ed. M. E. Bailey & D. A. Williams (Cambridge: Cambridge Univ. Press), 449
Mathis, J. S. 1990, ARA&A, 28, 37
McCall, M. L., Rybski, P. M., & Shields, G. A. 1985, ApJS, 57, 1
Natta, A., & Panagia, N. 1984, ApJ 287, 228
Osterbrock, D. E. 1989, Astrophysics of Gaseous Nebulae and Active Galactic Nuclei (Mill Valley: University Science Books)
Pastoriza, M. G. 1975, ApSS, 33, 173
Pei, Y. C., Fall, S. M., & Bechtold, J. 1991, ApJ 395, 130
Reif, R., Mebold, V., Goss, W. M., Van Woerden, H., & Sieman, B. 1982, A&AS, 50, 451
Seaton, M. J. 1979, MNRAS, 187, 73P
Sérsic, J. L., & Pastoriza, M. 1965, PASP, 77, 287
Storchi-Bergmann, T., Calzetti, D., & Kinney, A. L. 1994a, ApJ, in press
Storchi-Bergmann, T., Kinney, A. L., & Challis, P. 1994b, in preparation
Witt, A. N., Bohlin, R. C., & Stecher, T. P. 1984, ApJ, 279, 698
Witt, A. N., Thronson, H. A., & Capuano, J. M. 1992, ApJ, 393, 611